

Elementary excitations of liquid ^4He in aerogel

O. Plantevin and B. Fåk

*Commissariat à l'Energie Atomique, Département de Recherche Fondamentale sur la Matière Condensée, SPSMS/MDN,
38054 Grenoble, France*

H. R. Glyde*

Institut Laue-Langevin, 156 X, 38042 Grenoble, France

J. Bossy

Centre de Recherches sur les Très Basses Températures, CNRS, BP 166, 38042 Grenoble, France

J. R. Beamish

Department of Physics, University of Alberta, Edmonton, Alberta, Canada T6G 2J1

(Received 5 November 1997)

The phonon-roton excitations of liquid ^4He immersed in aerogel of 95% porosity have been measured using inelastic neutron scattering. Excitations having wave vectors at the phonon ($Q=0.2 \text{ \AA}^{-1}$), maxon, roton, and beyond the roton ($Q=2.4 \text{ \AA}^{-1}$) regions of the dispersion curve were investigated at temperatures between $T=0.5 \text{ K}$ and $T=2.25 \text{ K}$. Aerogel grown with deuterated materials not exposed to air was used and measurements in bulk liquid ^4He were made under the same conditions for direct comparison. $S(Q, \omega)$ in ^4He in aerogel is very similar to that in bulk ^4He . There is no evidence for any low-energy excitations below the phonon-roton curve or of an energy gap in the dispersion curve ω_Q at small Q values. At $T=0.5 \text{ K}$ and at the maxon, roton, and at $Q=2.4 \text{ \AA}^{-1}$, the ^4He excitation energies ω_Q in aerogel lie a few μeV below the bulk values and the width Γ_Q of $S(Q, \omega)$ has a small finite value ($\Gamma_Q \sim 5 \mu\text{eV}$). The temperature dependence of the energies ω_Q and widths Γ_Q are similar, but not identical, to those in the bulk. [S0163-1829(98)01218-1]

I. INTRODUCTION

Bosons in disorder and confining environments display a rich spectrum of phases, transitions between phases, and novel flow properties.¹⁻³ A central example is liquid ^4He immersed in aerogel and vycor, which both confine the Bose liquid and introduce disorder.⁴⁻⁷ In these environments the universality class of the superfluid to normal transition is changed from the bulk and depends on the nature of the disorder, as does the transition temperature T_λ and the superfluid density $\rho_S(T)$ below T_λ .⁷ A second example is flux lines in dirty superconductors in which substitutional impurities or columnar line defects introduce disorder.⁸⁻¹¹ In this case the melting of the flux line lattice is substantially changed by the disorder, and the ordered Abrikosov flux line lattice, which is usually the low-temperature phase, is replaced by a flux line glass.^{2,12-17} Other important examples are the superconducting-insulator transitions in Josephson junction arrays,¹⁸⁻²⁰ in disordered thin films, and in granular metals.^{21,22} Of special interest is the nature of the excitations and the flow properties of bosons in disordered materials. Superfluid flow and sound propagation in liquid ^4He is qualitatively changed by disorder.⁷ The flow and elastic properties of flux lines in disorder determines the critical current properties of high- T_c superconductors.⁸ The flow of bosons in disorder has applications in charge density wave systems,²³⁻²⁶ Wigner crystals,²⁷ magnetic bubble arrays,²⁸ flow of vortices in Josephson junction arrays,²⁶ transport in metallic dots,²⁹ and flow in porous media generally.

The theoretical description of these systems is also a challenge because both the boson-boson interaction and disordering interaction must be included in the simplest models.^{1,3}

Direct simulation of bosons in a lattice containing a random potential have revealed important features.^{30,31} In these simulations, the type of the equilibrium phase is often identified by the magnitude of $\rho_S(T)$ and the nature of the elementary excitation spectrum ω_Q .³⁰ For example, a gap in ω_Q at $Q \rightarrow 0$ signals localization of the bosons by the disorder. Gaussian variational and renormalization group methods^{16,32} have identified important universal features of the phase transitions in disorder. The analysis of flow in disorder is an especially active topic.^{17,24,33,34}

In this paper, we report inelastic neutron-scattering measurements of the dynamic response and the elementary excitations of superfluid and normal ^4He in aerogel. The aim is to search for new features in the response introduced by the aerogel; for example, whether there are additional excitations at low energies ω as suggested in model calculations,³¹ whether there could be a gap in ω_Q at $Q \rightarrow 0$ in the superfluid or normal phases suggesting Mott localization,³⁰ whether the sound velocity is reduced by disorder as has been predicted,^{30,35} and whether the elementary excitations have a finite life time at low temperatures in disorder.

In a major program, excitations in liquid ^4He films up to 6–7 layers thick have been measured by inelastic neutron scattering.³⁶ These display a ripplon mode on the film surface-gas interface, a mode within the film similar to the phonon-roton mode in the bulk, and layer modes associated with the more tightly bound layers adjacent to the substrate on which the film resides. The structure of these films and the mode energies can be accurately predicted microscopically. An integrated account of the experiment and the calculations has recently appeared.³⁷

Inelastic neutron-scattering measurements of the excita-

tions of liquid ^4He in completely filled aerogel have been performed by two groups. Coddens and co-workers^{38,39} found that the excitation energies at $T \geq 1.5$ K were the same as in the bulk within the precision of their measurements. In the studies by Sokol, Gibbs, and co-workers,⁴⁰⁻⁴² which were extended to $T = 1.3$ K and covered the wave vector range $0.8 < Q < 2.1 \text{ \AA}^{-1}$, the excitation energies were found to be the same as in the bulk at low temperatures ($T = 1.3$ K). However, the temperature dependence of ω_Q differed from the bulk, especially at the roton wave vector, and the width of the excitations was larger than in the bulk at low temperatures. From the temperature dependence of the roton energy, the superfluid density $\rho_S(T) = 1 - \rho_N(T)$ was calculated using the Landau expression for $\rho_N(T)$ arising from thermal excitations of rotons.

We have measured the dynamic structure factor $S(Q, \omega)$ over a wide range of wave vectors, from $Q = 0.2 \text{ \AA}^{-1}$ in the phonon region to $Q = 2.4 \text{ \AA}^{-1}$ beyond the roton wave vector. We also covered a wide temperature range, from $T = 0.5$ K in the superfluid phase to $T = 2.25$ K in the normal phase. We make direct comparison with $S(Q, \omega)$ in bulk ^4He and have included measurements in the bulk under the same experimental conditions as a reference. In particular, we extract the energy ω_Q , width Γ_Q , and weight Z_Q of the single-excitation component in $S(Q, \omega)$ and compare the temperature dependence of these quantities with that of bulk ^4He , and whether Z_Q can be related to $\rho_S(T)$ as is apparently the case in the bulk.⁴³⁻⁴⁵

In Sec. II we describe the experiment and the aerogel sample. The results are presented in Sec. III and are discussed in relation to theoretical predictions and other data in Sec. IV.

II. EXPERIMENTAL

The measurements were performed on the IN12 cold neutron triple-axis spectrometer at the high-flux reactor of the Institut Laue-Langevin. A vertically focusing pyrolytic graphite (PG) (002) monochromator and a flat PG (002) analyzer were used. The horizontal collimations were $37'$, $38'$, $38'$, and $60'$ in order from monochromator to detector. The spectrometer was operated with a fixed final wave vector of $k_f = 1.4 \text{ \AA}^{-1}$. A 10-cm-thick liquid-nitrogen-cooled beryllium filter was used to remove higher-order neutrons from the scattered beam. Scans in energy were performed for wave vectors Q of 0.2, 1.1, 1.92, and 2.4 \AA^{-1} at temperatures T of 0.5, 1.4, 1.7, 1.85, 2.0, and 2.25 K. The energy resolution is nearly independent of energy transfer, and was 0.11 meV for elastic scattering and 0.12 meV at the maxon.

The aerogel sample was prepared using a standard one step tetramethoxysilane (TMOS) process, followed by hypercritical drying.⁴⁶ The amount of methanol in the solution was adjusted to give a final porosity of about 95%. The gel was grown under basic conditions using twice the stoichiometric amount of water. Similar base-catalyzed aerogels have been used in previous studies of aerogel structure and properties⁴⁷ and of superfluidity in aerogels.⁵ The aerogel was grown directly in the cell used for the neutron-scattering measurements, a 13.6-mm inner diameter stainless steel cylinder with a wall thickness of 0.2 mm and a height of 52 mm. Since base-catalyzed aerogels shrink very little during drying, there

were no visible gaps between the aerogel and the cell walls, i.e., no bulk helium is expected to be observed in the measurements.

In order to reduce the elastic scattering from the aerogel, of which a substantial fraction is believed to originate from OH^- groups attached to the aerogel strands, all the starting chemicals (TMOS, water, methanol, and ammonium hydroxide catalyst) were fully deuterated. From the starting purity of the chemicals, we estimate a residual H/D ratio for our samples of less than 1%. Care was taken to never expose the aerogel sample to air, since its surface would adsorb water. Samples were flushed with helium gas while still in the autoclave and were removed and sealed for transport under an argon atmosphere. All subsequent handling was made either under vacuum or under an inert gas atmosphere. In comparison with earlier neutron-scattering measurements,^{40,42} it appears that this substantially reduces the elastic scattering as discussed below.

The aerogel sample was not removed from the cell for characterization, but aerogels made under similar conditions had porosities (determined from the density) of 94%. Elastic neutron-scattering measurements down to $Q = 0.02 \text{ \AA}^{-1}$ were performed on IN12. The structure of the present aerogel is the same as observed in other base-catalyzed aerogels using small-angle x-ray and neutron scattering,⁴⁸ with a fractal exponent of $D = 1.8$.

High-purity ^4He was condensed into the aerogel-filled cell, which was mounted in a circulating ^3He cryostat. The sample temperature, measured by a calibrated carbon resistor, was stable within 5 mK. All measurements were performed at saturated vapor pressure. The scattering from the empty cell (aerogel only), measured at low temperatures for each wave vector, shows an elastic peak and an approximately flat background. A point-by-point subtraction was used for the elastic peak ($|\omega| < 0.2$ meV), and a constant background was subtracted outside the elastic-peak region. The data were normalized with respect to the beam monitor, after correction for the higher-order contamination in the incident beam. The absolute normalization was made with respect to previous measurements,^{45,49} and the resulting (resolution broadened) $S(Q, \omega)$ has units of meV^{-1} . Typical examples are shown in Figs. 1-4.

Since previous neutron-scattering measurements indicate rather small changes of the scattering from ^4He in aerogel compared with the bulk, the scattering from bulk ^4He condensed in a cell with identical dimensions was measured for each wave vector at the lowest temperature ($T = 0.5$ K) under conditions identical to those for the aerogel sample, at the end of the aerogel experiment. In this way, it is not necessary to rely on the absolute energy calibration of the spectrometer in order to determine the shift of the peak in $S(Q, \omega)$ due to the aerogel. Another advantage of doing the bulk measurements under identical conditions to the aerogel is that the width measured at low temperatures in the bulk gives directly the instrumental resolution, since the intrinsic broadening of the sharp peak in bulk ^4He is negligible at $T = 0.5$ K.^{50,51}

In previous measurements on nondeuterated aerogel, a dispersionless feature at the roton energy was observed for all Q values, with an intensity of approximately 10% of the roton intensity.⁴² This feature is observed in the present mea-

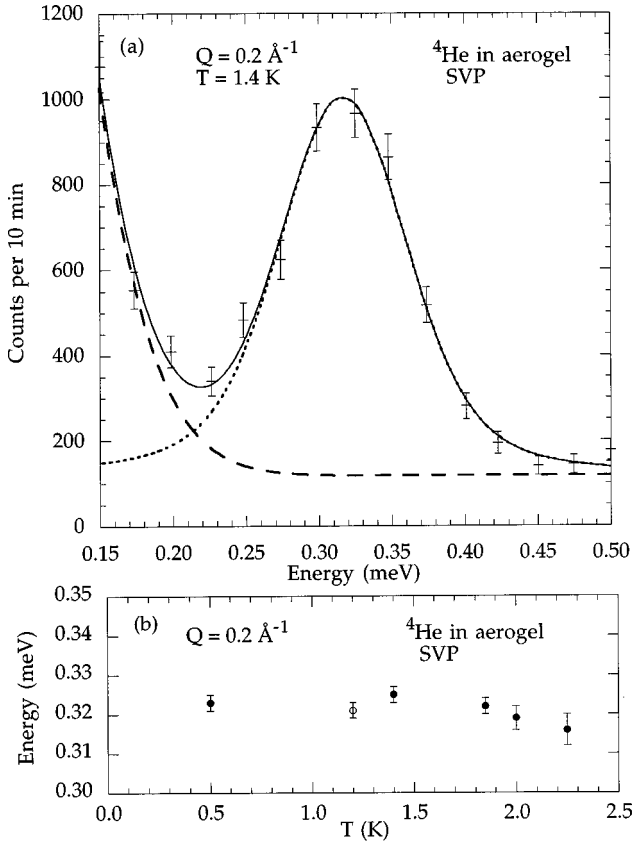


FIG. 1. (a) Raw spectra at the phonon wave vector $Q=0.2 \text{ \AA}^{-1}$ and $T=1.4 \text{ K}$. The long-dashed line shows the tail of the elastic scattering from the aerogel. (b) Temperature dependence of the phonon peak position for ^4He in aerogel (full circles) compared to bulk ^4He (open circle) (Ref. 52).

measurements on deuterated aerogel as well, but its intensity is reduced to only 1% of the roton intensity. This strongly suggests that the feature is due to multiple scattering, i.e., roton plus elastic scattering from the aerogel, as originally suggested by Gibbs *et al.*⁴² Since this multiple scattering probes the density of states of the helium scattering, it is expected to broaden with temperature, causing potential problems in analyzing the high-temperature data. The much smaller magnitude of the multiple scattering in the present experiment reduces this problem to a negligible level.

III. RESULTS

The measured $S(Q, \omega)$ from ^4He in aerogel is very similar to that in bulk ^4He . The only noticeable differences are in the shift and broadening of the sharp peak in $S(Q, \omega)$, both at low and high temperatures. These differences are very small, and models need to be fitted to the data in order to make the differences quantitative. The models are described in Sec. III A. The resulting fits to $S(Q, \omega)$ are shown in Sec. III B, where most of the data is presented. From the analysis in Sec. III A, we extract excitation energies, widths, and the weight of the intensity in the single excitation component of $S(Q, \omega)$ as a function of temperature, in Secs. III C, III D, and III E, respectively. At low temperatures, these quantities are well defined. However, at temperatures above 1.8 K they depend on how the data is analyzed, since the single-

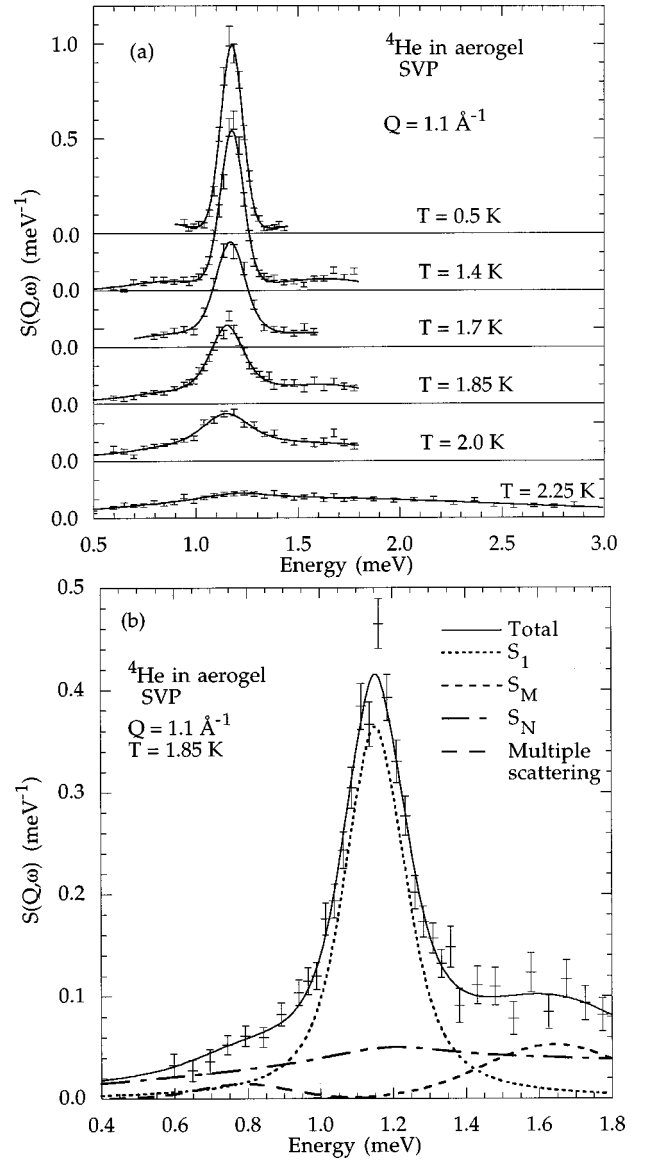


FIG. 2. (a) Temperature dependence of the dynamic structure factor at the maxon wave vector. The solid lines show the results of WS fits. The different components of the fits are detailed in (b) for $T=1.85 \text{ K}$.

excitation component of $S(Q, \omega)$ becomes rather broad.

A. Analysis

To analyze the data we have fitted the empirical relation for $S(Q, \omega)$, proposed by Woods and Svensson (WS)⁴³ for data in the bulk, to $S(Q, \omega)$ in aerogel. This is

$$S_{\text{WS}}(Q, \omega) = n_S S_S(Q, \omega) + n_N S_N(Q, \omega), \quad (1)$$

where $n_S = \rho_S / \rho$ and $n_N = \rho_N / \rho$ are the superfluid and normal fractions of the density, respectively, with $n_S + n_N = 1$. $S_N(Q, \omega)$ represents the broad scattering observed above T_λ , and $S_S(Q, \omega)$ is the sum of a sharp single excitation component, $S_1(Q, \omega)$, and a broad multiexcitation component $S_M(Q, \omega)$ that also exists at low temperatures,

$$n_S S_S(Q, \omega) = S_1(Q, \omega) + n_S S_M(Q, \omega). \quad (2)$$

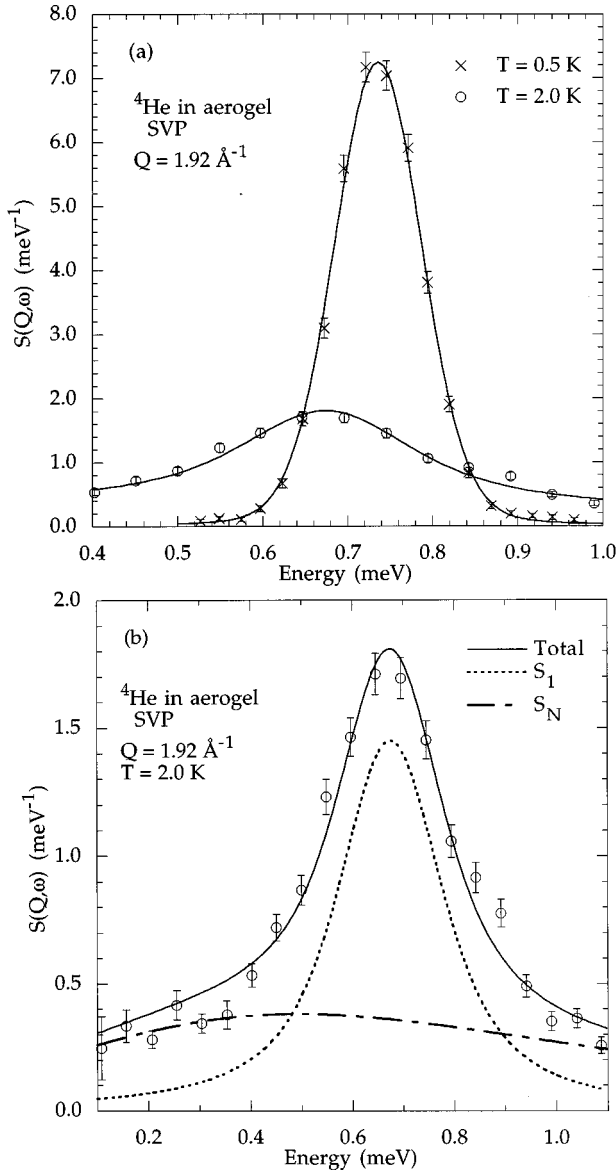


FIG. 3. (a) Dynamic structure factor at the roton wave vector at $T=0.5$ K and $T=2.0$ K. The solid lines show the results of WS fits. The different components of the fits are detailed in (b) for $T=2.0$ K.

The single excitation peak is represented by

$$S_1(Q, \omega) = \frac{1}{2\pi} \frac{1}{1 - \exp(-\hbar\omega/k_B T)} A_1(Q, \omega), \quad (3)$$

where

$$A_1(Q, \omega) = 2Z_Q \left[\frac{\Gamma_Q}{(\omega - \omega_Q)^2 + \Gamma_Q^2} - \frac{\Gamma_Q}{(\omega + \omega_Q)^2 + \Gamma_Q^2} \right] \\ = 2Z_Q \left[\frac{4\omega\omega_Q\Gamma_Q}{(\omega^2 - [\omega_Q^2 + \Gamma_Q^2])^2 + (2\omega\Gamma_Q)^2} \right]. \quad (4)$$

The response function $A_1(Q, \omega)$ can be equally expressed as the sum of two Lorentzians representing the Stokes and anti-Stokes processes or as a damped harmonic oscillator (DHO) function. In the first representation of $A_1(Q, \omega)$, ω_Q is identified as the excitation energy whereas in the second, Ω_Q

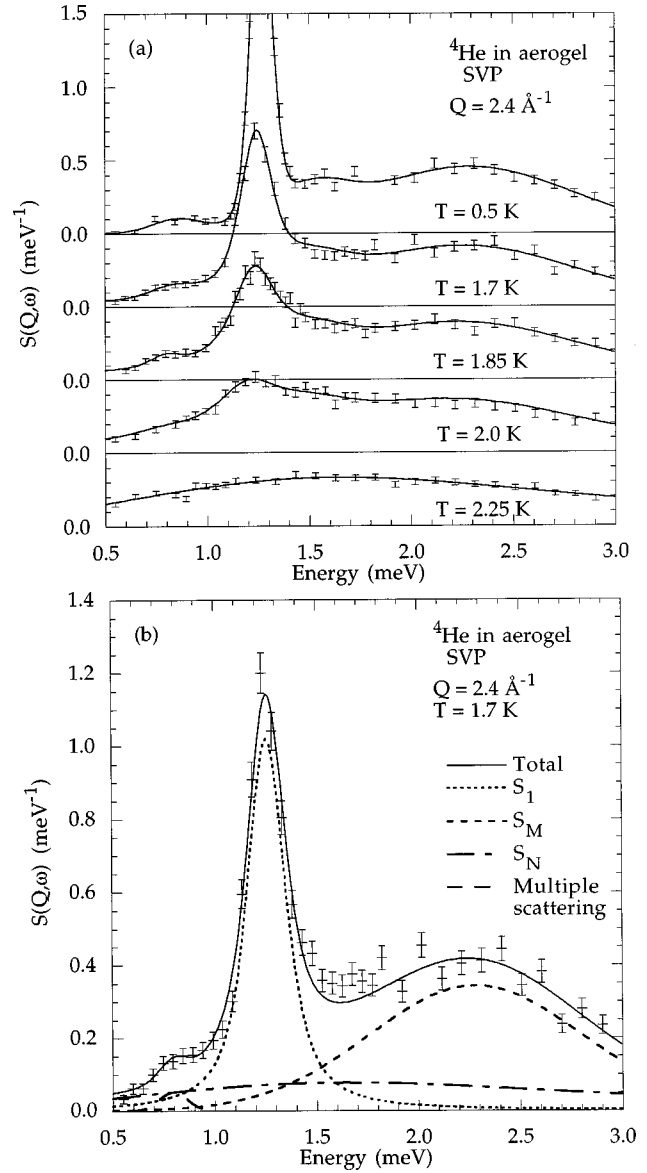


FIG. 4. (a) Temperature dependence of the dynamic structure factor at $Q=2.4$ \AA^{-1} . The solid lines show the results of the WS fits. The different components of the fits are detailed in (b) for $T=1.7$ K.

$= (\omega_Q^2 + \Gamma_Q^2)^{1/2}$ is often identified as the excitation energy. In this work we use ω_Q . Z_Q is the single-excitation weight, which is expected to scale with n_S .

At $T > T_\lambda$, where $n_N = 1$, $S_{WS}(Q, \omega)$ reduces to $S_N(Q, \omega)$. In the present analysis, $S_N(Q, \omega)$ is determined by fitting Eq. (1) to the broad $S(Q, \omega)$ observed at $T=2.25$ K. At the lowest temperature where $n_S = 1$, $S_{WS}(Q, \omega)$ reduces to $S_S(Q, \omega)$ which is determined by fitting to the observed $S(Q, \omega)$ at $T=0.5$ K. The shape of $S_N(Q, \omega)$ and $S_M(Q, \omega)$ are assumed to be temperature independent. Typical fits of the WS decomposition are shown in Figs. 2–4(a) for different Q values and selected temperatures. For temperatures up to about 1.8 K, $S_1(Q, \omega)$ is the dominating contribution, and it remains rather sharp. $S_M(Q, \omega)$ and $S_N(Q, \omega)$ are considerably weaker and broader than $S_1(Q, \omega)$. The multiple scattering component, observed at $Q=1.1$ and 2.4 \AA^{-1} , is even weaker, and is modelled by a Gaussian somewhat broader

than the resolution, since it reflects the density of states rather than the roton excitation. From these fits, the parameters for $S_1(Q, \omega)$, namely Z_Q , ω_Q , and Γ_Q , are extracted. The results are discussed in Sec. III C-E.

We have also analyzed the data using a second method, denoted the simple subtraction (SS) method. In this case the total scattering is represented by the sum of a single excitation component $S_1(Q, \omega)$ given by Eqs. (3), (4) and a multiexcitation component $S_m(Q, \omega)$,

$$S_{\text{SS}}(Q, \omega) = S_1(Q, \omega) + S_m(Q, \omega). \quad (5)$$

$S_m(Q, \omega)$ is assumed to be temperature independent, and is determined at the lowest temperature from $S(Q, \omega)$ after subtracting off $S_1(Q, \omega)$, which at low T is simply a resolution-broadened delta function. At higher temperatures, $S_1(Q, \omega)$ from Eqs. (3), (4) is fitted to the total $S(Q, \omega)$ after subtracting off $S_m(Q, \omega)$, with Z_Q , ω_Q , and Γ_Q as free parameters. This method gives the same excitation energies and widths as the WS method up to $T \approx 1.8$ K. For $T > 1.8$ K the SS method gives larger single excitation widths at the roton wave vector. Essentially, the intensity at the roton is entirely confined to a single peak at $T = 0.5$ K and $S_m(Q, \omega) \approx 0$. As a result, in the SS approach, $S_1(Q, \omega)$ is fitted to the total $S(Q, \omega)$ at $T = 0.5$ K and subsequently at all temperatures. In contrast, in the WS method, $S_1(Q, \omega)$ is fitted only to the peak region of the intensity, as shown in Fig. 3. Thus the WS method gives significantly narrower single excitation widths, which we believe better represent the elementary excitation width in the superfluid.

B. Dynamic structure factor

The general shape of the dynamic structure factor $S(Q, \omega)$ observed in aerogel is the same as observed in the bulk. We will here briefly describe $S(Q, \omega)$ for the four measured Q values.

Figure 1(a) shows raw data in the phonon region at $Q = 0.2 \text{ \AA}^{-1}$ and $T = 1.4$ K. The inelastic scattering from the sound mode is confined to a single peak centered at $\omega = 0.325$ meV. This peak sits on the tail of the elastic scattering from the aerogel, which extends to finite energies due to the instrumental resolution. The elastic scattering from the aerogel increases rapidly as Q decreases, and with the present aerogel sample it was not possible to measure phonons for smaller Q values than 0.2 \AA^{-1} . At $T = 0.5$ K and $Q = 0.2 \text{ \AA}^{-1}$, the peak is sharp (resolution limited) and as T increases the peak broadens. At $T = 1.4$ K, the width Γ_Q is $5.5 \mu\text{eV}$. As in the bulk, there remains a well defined peak above T_λ . Thus a sound mode propagates in normal liquid ^4He in aerogel as well as in the bulk. The mode energy at $Q = 0.2 \text{ \AA}^{-1}$ is approximately independent of temperature and has the same value as in the bulk [Fig. 1(b)].⁵² Therefore, if the phonon dispersion due to the aerogel is significantly modified at low wave vectors, this happens for $Q < 0.2 \text{ \AA}^{-1}$. From Fig. 1(a) we see also that there is no additional scattering at low energies beyond that in the symmetric resolution peak, at least for $\omega > 0.2$ meV. For $\omega < 0.2$ meV the intensity is dominated by elastic scattering

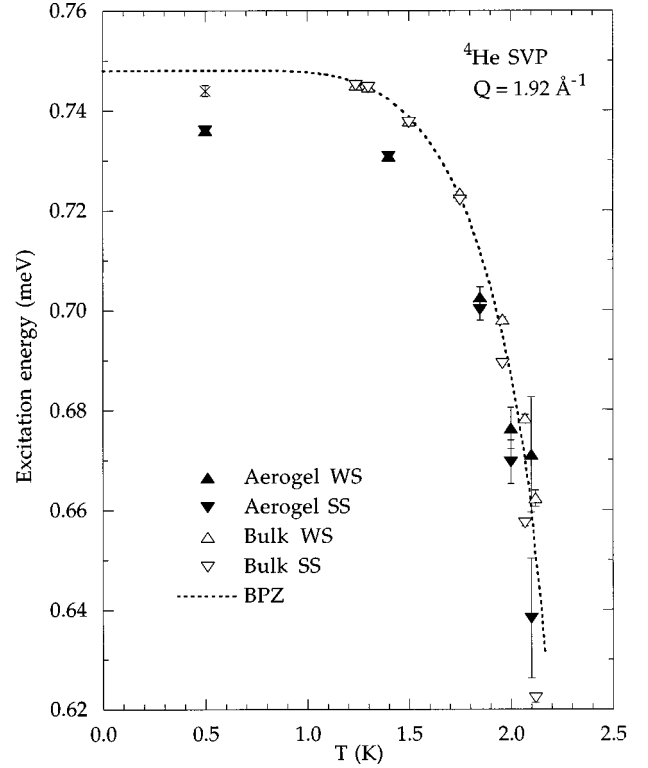


FIG. 5. Comparison of the roton energies obtained from the WS and SS methods both for ^4He in aerogel and for bulk ^4He .⁴⁵ Also shown is the roton energy in the bulk obtained from the present measurements at $T = 0.5$ K (cross). The dashed line is the BPZ expression Eq. (6).

from the aerogel. Because of this elastic scattering, it will be difficult in future experiments to investigate Q values less than 0.2 \AA^{-1} .

Figure 2(a) shows the temperature dependence of $S(Q, \omega)$ at the maxon wave vector $Q = 1.1 \text{ \AA}^{-1}$. As in the bulk, the sharp peak at low temperatures, centered at $\omega = 1.18$ meV, broadens with increasing temperature and its intensity drops quickly. There is a substantial amount of multiexcitations $S_m(Q, \omega)$ as shown in Fig. 2(b). In the roton region, $Q = 1.92 \text{ \AA}^{-1}$, $S_m(Q, \omega)$ is negligible, as the intensity is confined almost entirely within a single peak centered at $\omega = 0.736$ meV at $T = 0.5$ K [Fig. 3(a)]. Thus at higher temperatures, $S(Q, \omega)$ consists of $S_1(Q, \omega)$ and $n_N S_N(Q, \omega)$ [see Fig. 3(b)].

Figure 4(a) shows $S(Q, \omega)$ observed at $Q = 2.4 \text{ \AA}^{-1}$ at different temperatures. At low temperatures, $S(Q, \omega)$ contains a sharp peak centered at $\omega = 1.24$ meV that can be identified as $S_1(Q, \omega)$. However, the component that is identified as the multiexcitation component $S_m(Q, \omega)$ in the WS method [Fig. 4(b)], is here stronger (in integrated intensity) than $S_1(Q, \omega)$. The contribution from multiple scattering is seen at energies of about 0.8 meV, i.e., below the peak in $S_1(Q, \omega)$. The temperature dependence of $S(Q, \omega)$ at all these Q values is the same as in the bulk.

C. Excitation energies

Figure 5 shows the single excitation energies at the roton wave vector in aerogel and in the bulk obtained from the present measurements and in the bulk measurements by

Andersen *et al.*⁴⁵ The energies obtained by fitting the WS and SS expressions agree up to $T=1.8$ K but the two differ at higher temperatures. This is found in both the aerogel and the bulk, and can be understood from the discussion of the two methods in Sec. III A. For reasons given there, we retain the WS fitting procedure for the rest of this paper. Figure 5 shows also that the roton energy is systematically lower in aerogel than in bulk, by about 8 ± 2 μeV . Since our bulk measurements at the lowest temperature ($T=0.5$ K) are made using the same spectrometer under identical conditions as the aerogel measurements, no systematic errors should enter here, and the difference is most likely a physical effect. Previous precision measurements^{52,53} of the roton energy Δ in the bulk provide a reference value $\Delta=0.742 \pm 0.001$ meV (8.61 ± 0.01 K).

To display the temperature dependence of the excitation energies, we have plotted the shift $\delta_Q(T) = \omega_Q(T) - \omega_Q(0)$ for both aerogel and the bulk in Fig. 6 for $Q=1.1$, 1.92 , and 2.4 \AA^{-1} . For comparison, the aerogel results of Gibbs *et al.*⁴² for the roton wave vector are also given. The present data suggest that there is no clear difference between the temperature dependence of the energies in aerogel and the bulk. The temperature dependence of the roton shift follows quite well the Bedell-Pines-Zawadowski (BPZ) expression⁵⁴

$$-\delta_Q(T) = 2.130(1 + 0.0603T^{1/2})T^{1/2}\exp[-\Delta(T)/k_B T] \quad (6)$$

as shown by the dotted line in Fig. 6(b). This expression describes a four-quasiparticle process in which the observed roton [of energy $\Delta(T)$] is scattered by a thermally excited roton to form two other quasiparticles, thus modifying the roton energy and introducing a finite life time (see below), as first discussed by Landau and Khalatnikov.⁵⁵ The shift and the broadening are here proportional to the number of thermally excited rotons. For the maxon and $Q=2.4$ \AA^{-1} , Eq. (6) is not valid, and we use the empirical expression

$$-\delta_Q(T) = \alpha T^{1/2}\exp(-\beta/k_B T) \quad (7)$$

to fit the bulk data with α and β as free (and temperature independent) parameters, as shown by the line in Figs. 6(a) and 6(c).

D. Excitation widths

Figure 7 compares the intrinsic width $\Gamma_Q(T)$ of the roton using the SS and the WS fitting procedures discussed in Sec. III A. The $\Gamma_Q(T)$ represents the half width at half maximum of the part of $S(Q, \omega)$ that is attributed to the single excitation response. For $T > 1.5$ K, the width $\Gamma_Q(T)$ in both the bulk and in aerogel obtained using the SS method are much larger than those obtained using the WS method. As discussed in Sec. III A, we believe that the WS widths better represent the width of the single excitation, and this one is used hereafter.

Figure 8 shows the single excitation width $\Gamma_Q(T)$ for both aerogel and bulk at $Q=1.1$, 1.92 , and 2.4 \AA^{-1} . For comparison, the aerogel results of Gibbs *et al.*⁴² for the maxon and roton are also given. The key feature in aerogel is that $\Gamma_Q(T)$ appears to saturate at a constant value for temperatures below $T \approx 1$ K, whereas $\Gamma_Q(T)$ in the bulk decreases without

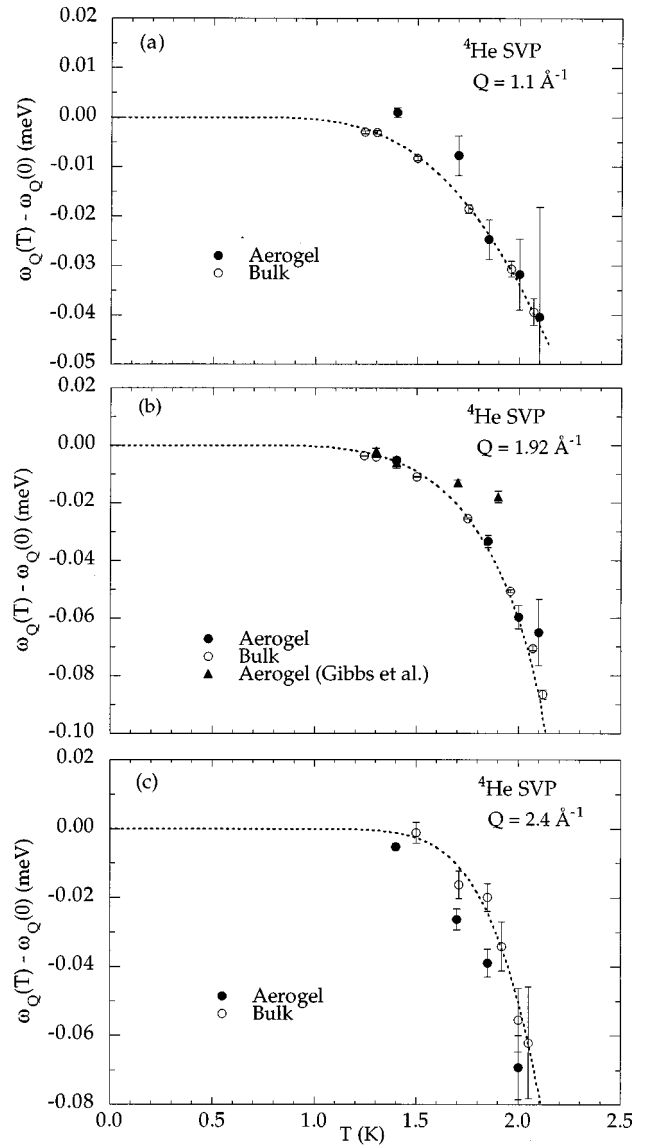


FIG. 6. Temperature dependence of the shifts of the excitation energies both for ${}^4\text{He}$ in aerogel and for bulk ${}^4\text{He}$ ^{45,49} at $Q=1.1$, 1.92 , and 2.4 \AA^{-1} . At the roton, the dotted line is the BPZ expression Eq. (6) and the triangles are aerogel results from Gibbs *et al.* (Ref. 42). At $Q=1.1$ and 2.4 \AA^{-1} , the lines are fits of the empirical expression Eq. (7) for the bulk, to guide the eyes.

limit. The constant value is 3 ± 2 μeV , 6 ± 1 μeV , and 7 ± 1 μeV at $Q=1.1$, 1.92 , and 2.4 \AA^{-1} , respectively.

In principle, some of this width could arise from multiple scattering. Scattering from excitations having Q values in the immediate vicinity of the selected Q can be redirected into the selected Q via a second elastic scattering event from the aerogel. If these neighboring excitations have a different energy, a broadened peak is observed. At the maxon, the peak would broaden towards lower energies, since neighboring excitations have lower energies. At the roton, the broadening would be on the high-energy side of the peak. We observed symmetric peaks at both the maxon and the roton, which were broader on both sides of the bulk reference peaks, except for the shift to lower energies discussed in Sec. III C [Fig. 9(a)]. By shifting the aerogel data to higher energies and increasing its intensity [Fig. 9(b)], the broadening is ap-

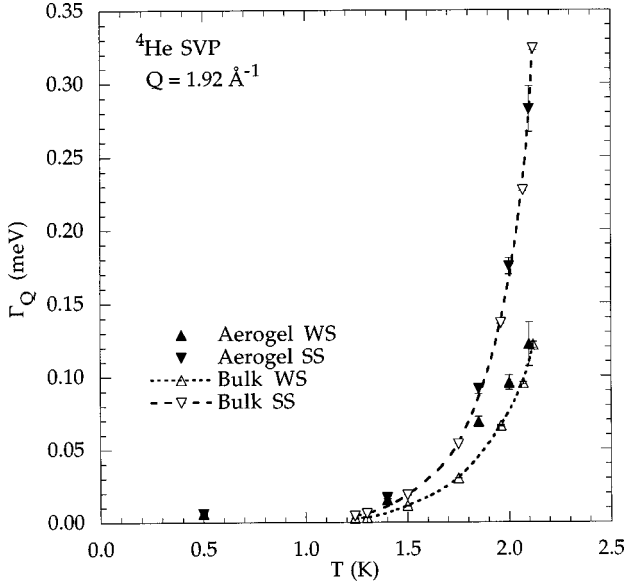


FIG. 7. Comparison of the roton widths half width at half maximum (HWHM) obtained from the WS and SS methods both for ^4He in aerogel and for bulk ^4He (Ref. 45). The dotted lines are guides to the eyes.

parent to the naked eye without any fitting. Gibbs *et al.* found in their Monte Carlo simulations that multiple scattering would not give rise to any excitation broadening.⁴² This conclusion, if correct, would be valid even in our case, since the multiple scattering is much less in our deuterated aerogel. However, we cannot exclude that part or all of the broadening is due to multiple scattering.

The roton line width in the bulk is reasonably well described by the BPZ expression⁵⁴

$$\Gamma_Q(T) = 3.585(1 + 0.0603T^{1/2})T^{1/2}\exp[-\Delta(T)/k_B T] \quad (8)$$

[dashed line in Fig. 8(b)]. At the maxon and at $Q = 2.4 \text{ \AA}^{-1}$, the empirical expression

$$\Gamma_Q(T) = \alpha T^{1/2} \exp(-\beta/T) \quad (9)$$

can be fitted to the bulk data, with α and β as free and temperature independent parameters [dashed lines in Figs. 8(a) and 8(c)]. In the aerogel, the same expressions can be used up to $T \approx 1.85 \text{ K}$ if a constant value is added: $3.5 \mu\text{eV}$ at $Q = 1.1 \text{ \AA}^{-1}$, $6 \mu\text{eV}$ at $Q = 1.92 \text{ \AA}^{-1}$, and $7 \mu\text{eV}$ at $Q = 2.4 \text{ \AA}^{-1}$ (solid lines in Fig. 8).

E. Single excitation intensity

Figure 10 shows the parameter $Z_Q(T)$ that characterizes the intensity in the single excitation component of $S(Q, \omega)$, obtained using the WS method. Also shown is the observed superfluid density in the bulk multiplied by a constant factor to best fit the data. To implement the WS method, we have used the observed values of the normal density n_N in $n_N S_N(Q, \omega)$. As discussed by Mineev⁵⁶ and Talbot *et al.*,⁴⁴ the use of the observed bulk normal density in $n_N S_N(Q, \omega)$ will lead to a $Z_Q(T)$ that must scale as the bulk superfluid density if the total static structure factor $S(Q)$ is independent of T . In bulk ^4He , $S(Q)$ for $Q \geq 1.1 \text{ \AA}^{-1}$ is constant within

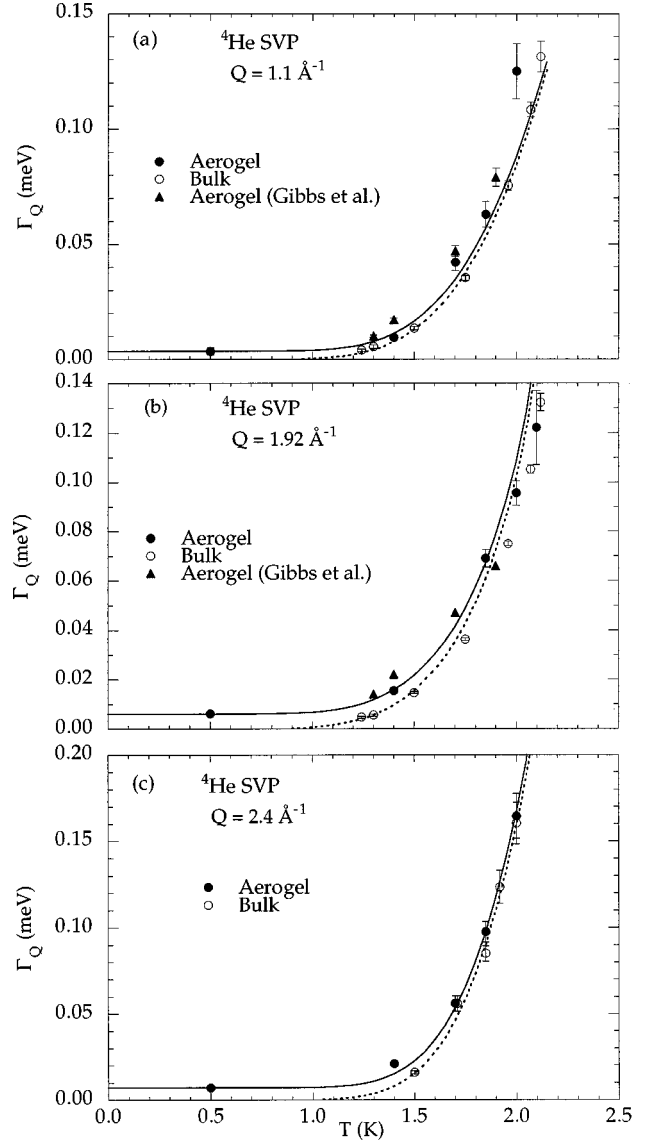


FIG. 8. Temperature dependence of the widths Γ_Q (HWHM) both for ^4He in aerogel [from the present measurements and from Gibbs *et al.* (Ref. 42)] and for bulk ^4He (Refs. 45, 49) at $Q = 1.1$, 1.92 , and 2.4 \AA^{-1} . At the roton, the dotted line is the BPZ expression Eq. (8). At $Q = 1.1$ and 2.4 \AA^{-1} , the dotted lines are fits of the empirical expression (9) for the bulk. The solid lines are equal to the dotted lines plus a constant value (see text).

2–4 % between $T = 0 \text{ K}$ and T_λ .⁵⁷ From Fig. 10 we see that $Z_Q(T)$ does indeed scale as the bulk n_S , except perhaps at the roton where there is a deviation from n_S at intermediate temperatures. Otherwise $Z_Q(T)$ scales with n_S as in the bulk within observed precision.

IV. DISCUSSION

Aerogels have a highly tenuous structure of irregularly connected silica strands. A typical aerogel with a porosity of 95% (i.e., silica occupying a fraction $f = 0.05$ of the sample) has a specific surface area of about 600 m^2 per gram. From the area per unit volume $A/V = 0.65 \times 10^6 \text{ cm}^{-1}$, an average strand diameter (assuming cylindrical strands) can be determined, $D = 4f(V/A) = 32 \text{ \AA}$. Typical spacing between

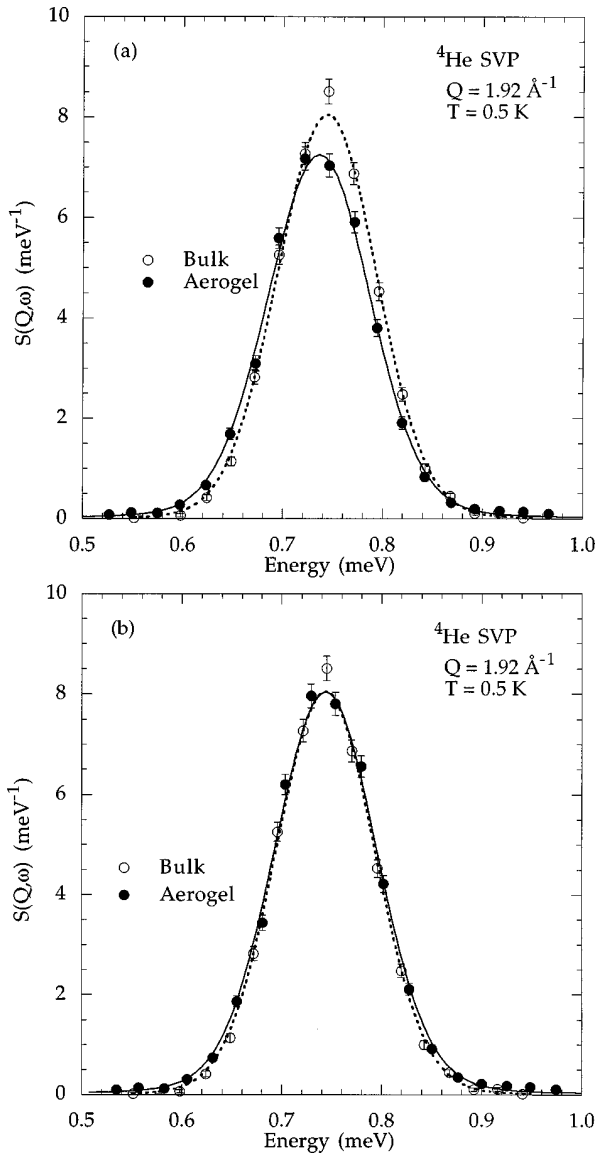


FIG. 9. (a) Dynamic structure factor of ${}^4\text{He}$ in aerogel and of bulk ${}^4\text{He}$ at the roton at $T=0.5$ K. The figure shows the shift of the roton excitation. (b) Same data, but where the aerogel data have been shifted in energy and multiplied by a scale factor such that the peak position and peak height are the same as for the bulk data. This allows to visualize the broadening of the peak in aerogel. The dashed line is a Gaussian fit to the bulk data, and the solid line is a fit to the aerogel data of Eqs. (3), (4) folded with the instrumental resolution.

strands can be estimated as $d=(4\pi f)^{1/2}(V/A)=125\text{ \AA}$. Small-angle scattering, transmission-electron microscope images, and desorption measurements on similar aerogels show a distribution of pore length scales from a few to a few hundred \AA . The first two layers of ${}^4\text{He}$ on the aerogel are expected to be solidlike. The aerogel plus the solid ${}^4\text{He}$ layers bound to it may be viewed as strands of an elastic medium having a different elastic constant traversing bulk liquid ${}^4\text{He}$ in a random manner. The mean free path in this environment is typically $l\sim 4(V/A)\sim 700\text{ \AA}$ or 1000 \AA .⁵⁸ This is much longer than the wavelength of the excitations investigated here.

From Fig. 1(b) we see that the energy of a phonon at Q

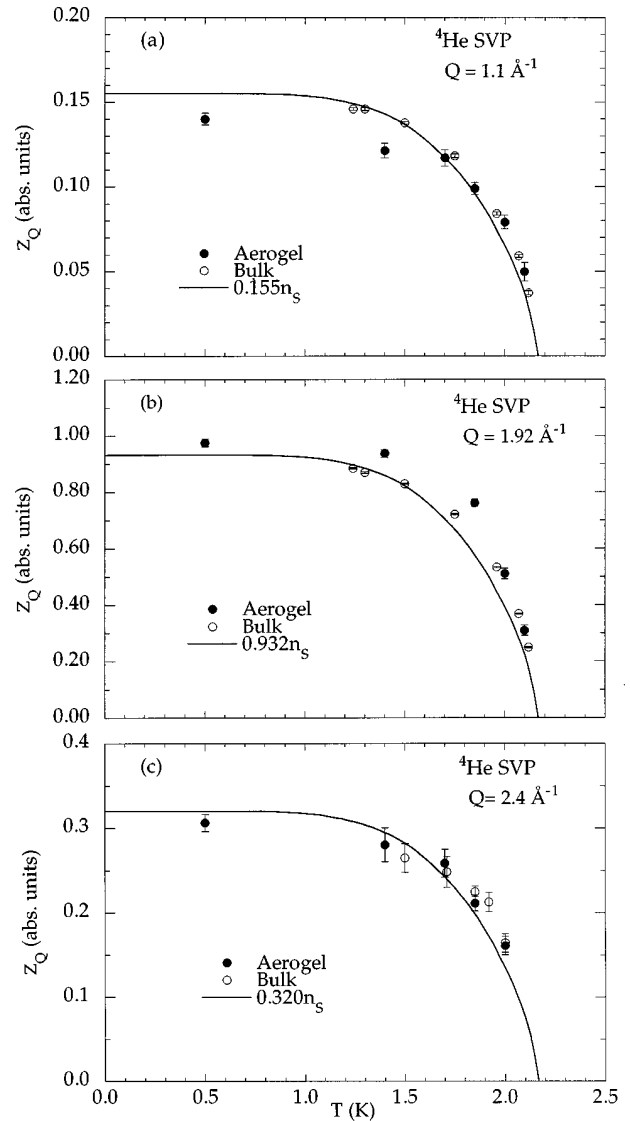


FIG. 10. Temperature dependence of the intensity of the single excitation component (WS decomposition) at $Q=1.1$, 1.92 , and 2.4 \AA^{-1} both for ${}^4\text{He}$ in aerogel and for bulk ${}^4\text{He}$ (Refs. 45, 49). The solid lines are proportional to the superfluid density in the bulk, with a scale factor as indicated.

$=0.2\text{ \AA}^{-1}$ propagating in this sample is independent of temperature between $T=0.5$ and $T=2.25$ K and is the same as in pure bulk liquid ${}^4\text{He}$ within precision. Thus we observe that the sound velocity c , defined by $\omega_Q=cQ$, is unchanged from the bulk and is the same in the superfluid and normal phases. Zhang³⁵ has evaluated the sound velocity of a dilute Bose gas in a weak random potential within the Bogoliubov approximation. He found that the sound velocity of the Bogoliubov phonons is reduced by disorder with a reduction proportional to the square of the variance of the random interface. To leading order, the width of the phonon is not changed by the disorder. For bosons in a 2D lattice, Krauth *et al.*³⁰ find c is reduced by a random potential. At the present degree of disorder and at the $Q=0.2\text{ \AA}^{-1}$ investigated, no reduction of c is observed here. However, at higher wave vectors, at the maxon, roton, and at $Q=2.4\text{ \AA}^{-1}$, ω_Q was shifted to lower values in aerogel.

Makivic *et al.*³¹ simulated bosons on a 2D lattice subject

to a random site potential. Their results suggested there were additional excitations at low energy (ω) induced by disorder in this system. Such excitations would appear as additional weight at low ω in $S(Q, \omega)$ in the present sample. We do not find additional intensity in $S(Q, \omega)$ at low ω at any wave vector. From Fig. 1(a) we see that $S(Q, \omega)$ at $Q=0.2 \text{ \AA}^{-1}$ is dominated by elastic scattering from the aerogel in the low ω ($\omega \approx 0$) region. The elastic scattering from the present aerogel sample is significantly smaller than that observed in previous measurements.^{38–42} Indeed, as noted in Sec. II, special care was taken to prepare the aerogel using deuterated materials and not to expose the aerogel to air to reduce the hydrogen content and adsorbed impurities. For this reason, and given the nature of the elastic scattering from the aerogel shown in Fig. 1(a), it will be difficult to observe additional weight in $S(Q, \omega)$ at lower wave vectors and energies in future measurements. It is generally at low Q and ω that additional weight arising from disorder is most expected to occur.

If there is localization of the liquid, especially of the condensate, a gap in the dispersion curve at $Q \rightarrow 0$ is anticipated. Specifically, if the superfluid to normal transition is associated with localization by disorder, we anticipate a gap appearing in ω_Q in the normal phase. Since the phonon energy at $Q=0.2 \text{ \AA}^{-1}$ is independent of temperature and is the same as in bulk liquid ^4He , the present data do not suggest any gap formation in superfluid or normal ^4He induced by aerogel at 95% porosity.

While the phonon energy at $Q=0.2 \text{ \AA}^{-1}$ is approximately independent of temperature, the excitations energies at all higher wave vectors decrease significantly with increasing temperature for $T \geq 1 \text{ K}$ in both aerogel and in the bulk. To test whether this decrease was greater or less in aerogel than in the bulk, we have plotted the shift $\delta_Q(T) = \omega_Q(T) - \omega_Q(0)$ for the two cases in Fig. 6. There we see that in aerogel the decrease is less at the maxon, greater at $Q=2.4 \text{ \AA}^{-1}$, and the same at the roton as in the bulk within the present precision of measurements. Further measurements are needed to confirm whether this variation of $\delta_Q(T)$ with Q is significant or not. At the roton Q , Sokol, Gibbs, and co-workers^{41,42} found that $\omega_Q(T)$ decreased significantly less with increasing temperature in aerogel than in bulk liquid ^4He . Their aerogel sample also showed significantly more elastic scattering than the present sample. It is possible that the impact of the aerogel is greater in their case and that $\omega_Q(T)$ is not the same in the two samples. Further measurements are needed to explore the impact of different aerogels and of different exposure to air on $\omega_Q(T)$.

Bogoliubov⁵⁹ showed that the characteristic excitations of a dilute Bose gas, however weak the interaction, have energies of the phonon-roton form. The excitations in a dilute gas can be equally regarded as single quasiparticle or density excitations. Gavoret and Nozières⁶⁰ showed that the single quasiparticle and density excitations of a strongly interacting Bose fluid have the same energy spectrum and that the quasiparticle excitations appear as a component in $S(Q, \omega)$. Essentially, in a uniform Bose fluid there are no low-energy excitations under the phonon-roton curve to which the phonons or rotons can decay.⁶¹ As a result the phonon-roton lifetimes become infinite as $T \rightarrow 0$. These arguments hold equally for a nonuniform Bose gas confined or trapped in a

smooth potential.⁶² In the present sample, we observe a finite lifetime to the excitations at low temperature at the maxon, roton, and at $Q=2.4 \text{ \AA}^{-1}$. This life time could arise from the scattering of the phonon-roton excitations from the disorder, from surfaces, and from changes of elastic properties introduced by the aerogel.

Calculations and neutron-scattering measurements show that liquid ^4He on a substrate has a highly layered nature. Modes propagate in the individual layers often denoted ‘‘layer phonons.’’³⁷ These layer modes may be expected to exist in the ^4He layers adjacent to the aerogel in the present sample. The bulklike excitations observed here could scatter from the ‘‘layer phonons’’ leading to a finite width of the bulk excitations.

The aerogel could also introduce a density variation in the liquid. Since ^4He is attracted to the aerogel, the liquid ^4He density near the aerogel is likely to be higher than the SVP density. In bulk ^4He , the excitation energy is a sensitive function of pressure. For example, the roton energy decreases by approximately $100 \mu\text{eV}$ between SVP and 20 bar. This change results from the density increase. The change in the excitation energy with pressure is larger at the roton than at the maxon. In the present case a spectrum of energies would be observed resulting from scattering from different regions in the sample at different densities. The observed average $S(Q, \omega)$ would have a width. The observed half width of 3 and $6 \mu\text{eV}$ at the maxon and roton wave vectors, respectively, is not inconsistent with probable density variations in the sample. Further measurements are needed to confirm these widths and particularly their variation with Q .

As noted by Woods and Svensson,⁴³ the intensity in the single excitation peak, given by $Z_Q(T)$, scales with temperature approximately as the superfluid density $\rho_S(T)$ in bulk ^4He . An aim of the present measurement was to test whether or not this approximate scaling persisted in systems in which $\rho_S(T)$ is modified by disorder. One of the difficulties in carrying out such a test is finding a model-independent method of analyzing $S(Q, \omega)$. Here we have used the Woods and Svensson decomposition of $S(Q, \omega)$, exactly as used in the bulk, with $n_N(T) = \rho_N(T)/\rho = 1 - \rho_S(T)/\rho$ in $n_N(T)S_N(Q, \omega)$ given by the observed normal density of bulk ^4He . This provides a good general description of $S(Q, \omega)$ and its temperature dependence. We see also from Fig. 10 that $Z_Q(T)$ in the present aerogel sample scales with T as the bulk $n_S(T)$ within precision. Certainly the aerogel data, analyzed using exactly the same procedure as the bulk and using the bulk $n_N(T)$ as input in $n_N(T)S_N(Q, \omega)$, does not show any new features reflecting the different $\rho_S(T)$ in aerogel. At the same time, as noted above, if $S(Q)$ is constant and if the bulk $n_N(T)$ is used in $n_N(T)S_N(Q, \omega)$, then we expect the $Z_Q(T)$ to scale as the bulk $n_S(T)$. A more critical test of the temperature dependence of $Z_Q(T)$ is really needed. Microscopically, we expect $Z_Q(T)$ to be related to the condensate fraction.⁶¹

ACKNOWLEDGMENTS

This work was supported in part by the National Science Foundation through research Grant Nos. INT-9314661 and DMR-9623961. Valuable discussions with Dr. N. Mulders are gratefully acknowledged.

- *Permanent address: Department of Physics and Astronomy, University of Delaware, Newark, Delaware 19716.
- ¹D. J. Thouless, Phys. Rep., Phys. Lett. **13C**, 93 (1974).
 - ²M. P. A. Fisher, P. B. Weichman, G. Grinstein, and D. S. Fisher, Phys. Rev. B **40**, 546 (1989); M. P. A. Fisher, Phys. Rev. Lett. **62**, 1415 (1989).
 - ³M. Ma, P. Nisamaneephong, and L. Zhang, J. Low Temp. Phys. **93**, 957 (1993).
 - ⁴B. C. Crooker, E. Hebral, E. N. Smith, Y. Takano, and J. D. Reppy, Phys. Rev. Lett. **51**, 666 (1983).
 - ⁵M. H. W. Chan, K. I. Blum, S. Q. Murphy, G. K. S. Wong, and J. D. Reppy, Phys. Rev. Lett. **61**, 1950 (1988).
 - ⁶M. Larson, N. Mulders, and G. Ahlers, Phys. Rev. Lett. **68**, 3896 (1992).
 - ⁷J. D. Reppy, J. Low Temp. Phys. **87**, 205 (1992).
 - ⁸G. Blatter, M. V. Feigel'man, V. B. Geshkenbein, A. I. Larkin, and V. M. Vinokur, Rev. Mod. Phys. **66**, 1125 (1994).
 - ⁹H. Safer, P. L. Gammel, D. A. Huse, D. J. Bishop, W. C. Lee, J. Giapintzakis, and D. M. Ginsberg, Phys. Rev. Lett. **70**, 3800 (1993).
 - ¹⁰T. K. Worthington, M. P. A. Fisher, D. A. Huse, J. Toner, A. D. Marwick, T. Zabel, C. A. Feild, and F. Holtzberg, Phys. Rev. B **46**, 11 854 (1992).
 - ¹¹J. A. Fendrich, W. K. Kwok, J. Giapintzakis, C. J. van der Beek, V. M. Vinokur, S. Fleshler, U. Welp, H. K. Viswanathan, and G. W. Crabtree, Phys. Rev. Lett. **74**, 1210 (1995).
 - ¹²A. I. Larkin, Zh. Eksp. Teor. Fiz. **58**, 1466 (1970) [Sov. Phys. JETP **31**, 784 (1970)].
 - ¹³D. S. Fisher, M. P. A. Fisher, and D. A. Huse, Phys. Rev. B **43**, 130 (1991).
 - ¹⁴D. A. Huse and H. S. Seung, Phys. Rev. B **42**, 1059 (1990).
 - ¹⁵E. Bonabeau and P. Lederer, Phys. Rev. Lett. **77**, 5122 (1996).
 - ¹⁶T. Giamarchi and P. Le Doussal, Phys. Rev. Lett. **72**, 1530 (1994); Phys. Rev. B **52**, 1242 (1995).
 - ¹⁷S. Ryu *et al.*, Phys. Rev. Lett. **77**, 5114 (1996).
 - ¹⁸M. G. Forrester *et al.*, Phys. Rev. B **37**, 5966 (1988).
 - ¹⁹M. G. Forrester *et al.*, Phys. Rev. B **41**, 8749 (1990).
 - ²⁰D. C. Harris *et al.*, Phys. Rev. Lett. **67**, 3606 (1991).
 - ²¹M. C. Cha *et al.*, Phys. Rev. B **44**, 6883 (1991).
 - ²²A. van Otterlo *et al.*, Phys. Rev. B **48**, 3316 (1993).
 - ²³S. Bhattacharya *et al.*, Phys. Rev. Lett. **63**, 1503 (1989); S. Bhattacharya and M. J. Higgins, *ibid.* **70**, 2617 (1993); Phys. Rev. B **49**, 10 005 (1994).
 - ²⁴L. Balents and M. P. A. Fisher, Phys. Rev. Lett. **75**, 4270 (1995).
 - ²⁵G. Gruener, Rev. Mod. Phys. **60**, 1129 (1988).
 - ²⁶F. Falo *et al.*, Phys. Rev. B **41**, 10 983 (1990).
 - ²⁷M. C. Cha and H. A. Fertig, Phys. Rev. B **50**, 14 368 (1994).
 - ²⁸R. Seshadri and R. M. Westervelt, Phys. Rev. B **46**, 5142 (1992); **46**, 5150 (1992).
 - ²⁹A. A. Middleton and N. S. Wingren, Phys. Rev. Lett. **71**, 3198 (1993).
 - ³⁰W. Krauth and N. Trivedi, Europhys. Lett. **14**, 627 (1991); W. Krauth, N. Trivedi, and D. M. Ceperley, Phys. Rev. Lett. **67**, 2307 (1991).
 - ³¹M. Makivic, N. Trivedi, and S. Ullah, Phys. Rev. Lett. **71**, 2307 (1993).
 - ³²T. Giamarchi and P. Le Doussal, Phys. Rev. Lett. **76**, 3408 (1996).
 - ³³D. Dominguez, Phys. Rev. Lett. **72**, 3096 (1994).
 - ³⁴M. Dong *et al.*, Phys. Rev. Lett. **70**, 662 (1993).
 - ³⁵L. Zhang, Phys. Rev. B **47**, 14 364 (1993).
 - ³⁶H. J. Lauter *et al.*, Phys. Rev. Lett. **68**, 2484 (1992); J. Low Temp. Phys. **87**, 425 (1992).
 - ³⁷B. E. Clements *et al.*, Phys. Rev. B **53**, 12 242 (1996).
 - ³⁸J. de Kinder, G. Coddens, and R. Millet, Z. Phys. B **95**, 511 (1994).
 - ³⁹G. Coddens, J. de Kinder, and R. Millet, J. Non-Cryst. Solids **188**, 41 (1995).
 - ⁴⁰M. R. Gibbs *et al.*, Physica B **213–214**, 462 (1995).
 - ⁴¹P. E. Sokol *et al.*, Nature (London) **379**, 616 (1996).
 - ⁴²M. R. Gibbs, P. E. Sokol, W. G. Stirling, R. T. Azuah, and M. A. Adams, J. Low Temp. Phys. **107**, 33 (1997).
 - ⁴³A. D. B. Woods and E. C. Svensson, Phys. Rev. Lett. **41**, 974 (1978).
 - ⁴⁴E. F. Talbot, H. R. Glyde, W. G. Stirling, and E. C. Svensson, Phys. Rev. B **38**, 11 229 (1988).
 - ⁴⁵K. H. Andersen, W. G. Stirling, R. Scherm, A. Stunault, B. Fåk, H. Godfrin, and A. J. Dianoux, J. Phys.: Condens. Matter **6**, 821 (1994); K. H. Andersen and W. G. Stirling, *ibid.* **6**, 5805 (1994).
 - ⁴⁶See, e.g., *Sol-Gel Science, The Physics and Chemistry of Sol-Gel Science*, edited by C. J. Brinker and G. W. Scherer (Academic, London, 1990).
 - ⁴⁷T. Woignier, J. Phalippou, and R. Vacher, J. Mater. Res. **4**, 688 (1989).
 - ⁴⁸D. W. Schaefer and K. D. Keefer, Phys. Rev. Lett. **56**, 2199 (1986); R. Vacher, T. Woignier, J. Pelous, and E. Courtens, Phys. Rev. B **37**, 6500 (1988).
 - ⁴⁹B. Fåk and K. H. Andersen, Phys. Lett. A **160**, 468 (1991); B. Fåk, L. P. Regnault, and J. Bossy, J. Low Temp. Phys. **89**, 345 (1992); B. Fåk and J. Bossy, J. Low Temp. Phys. (to be published).
 - ⁵⁰F. Mezei, Phys. Rev. Lett. **44**, 1601 (1980).
 - ⁵¹K. H. Andersen, J. Bossy, J. C. Cook, O. G. Randl, and J. L. Ragazzoni, Phys. Rev. Lett. **77**, 4043 (1996).
 - ⁵²W. G. Stirling, in *75th Jubilee Conference on Helium-4*, edited by J. G. M. Armitage (World Scientific, Singapore, 1983), p. 109.
 - ⁵³A. D. B. Woods, P. A. Hilton, R. Scherm, and W. G. Stirling, J. Phys. C **10**, L45 (1977).
 - ⁵⁴K. Bedell, D. Pines, and A. Zawadowski, Phys. Rev. B **29**, 102 (1984).
 - ⁵⁵L. D. Landau and I. M. Khalatnikov, Zh. Eksp. Teor. Fiz. **19**, 637 (1949).
 - ⁵⁶V. P. Mineev, Pis'ma Zh. Eksp. Teor. Fiz. **32**, 509 (1980) [JETP Lett. **32**, 489 (1980)].
 - ⁵⁷E. C. Svensson, V. F. Sears, A. D. B. Woods, and P. Martel, Phys. Rev. B **21**, 3638 (1980).
 - ⁵⁸A. Emmerling and J. Fricke, J. Non-Cryst. Solids **145**, 113 (1992).
 - ⁵⁹N. N. Bogoliubov, J. Phys. (Moscow) **11**, 23 (1947).
 - ⁶⁰J. Gavoret and P. Nozières, Ann. Phys. (N.Y.) **28**, 349 (1964).
 - ⁶¹H.R. Glyde, *Excitations in Liquid and Solid Helium* (Oxford University Press, Oxford, 1994); J. Low Temp. Phys. **93**, 349 (1993).
 - ⁶²M. Edwards *et al.*, Phys. Rev. Lett. **77**, 1671 (1996); K. G. Singh and D. S. Rokhsar, *ibid.* **77**, 1667 (1996); D. A. W. Hutchinson *et al.*, *ibid.* **78**, 1842 (1997).